

Ribosomal Proteins Neighboring 23 S rRNA Nucleotides 803–811 within the 50 S Subunit[†]

Rebecca W. Alexander[‡] and Barry S. Cooperman*

Department of Chemistry, University of Pennsylvania, Philadelphia, Pennsylvania 19104-6323

Received September 12, 1997; Revised Manuscript Received December 5, 1997

ABSTRACT: We report the synthesis of a radioactive, photolabile oligodeoxyribonucleotide probe and its exploitation in identifying 50 S ribosomal subunit components neighboring its target site, nucleotides 803–811 in 23 S rRNA. Photolysis of the complex formed between the probe and 50 S subunits leads to site-specific probe photoincorporation into proteins L15, L17, and L20, labeled to greater extents, and L13 and L21, labeled to lesser extents. Portions of each of these proteins thus lie within 23 Å of nucleotide U803. These results lead us to conclude that nucleotides 803–811 fall on the side of the L13–L17–L20–L21 protein cluster [Walleczek et al. (1988) *EMBO J.* 7, 3571–3576] that points from the back of the 50 S particle toward the peptidyl transferase center within the 50 S subunit. Such placement is consistent with the observation that an oligoDNA probe directed to nucleotides 803–811 decreases P-site binding of tRNA [Hill et al. (1990) *Biochim. Biophys. Acta* 1050, 45–50].

We have been using radioactive photolabile oligoDNA probes, targeted toward functionally important regions of rRNA, to identify the ribosomal components that neighbor these rRNA regions (1–6). Such site-directed cross-linking studies provide the spatial constraints necessary for the construction of detailed three-dimensional models of ribosome structure and function (7, 8).

Nucleotides 803–811 are highly conserved within 23 S-like rRNAs. Hill et al. (9) have implicated this sequence in binding of the 3'-terminus of tRNA by demonstrating that an oligoDNA probe directed to nucleotides 803–811 decreased P-site binding of tRNA, while binding of tRNA lacking the 3'-CCA end was not affected, nor was the binding of intact tRNA to the A-site (9). Nucleotides 807–809 (UGG) had earlier been suggested as a possible binding site for the 3'-CCA terminus of tRNA (10). However, the subsequent finding that this sequence was not completely conserved (11) cast doubt on this suggestion, and recent experiments employing complementary mutations have provided strong evidence for a specific base-pairing interaction between C74 of P-site bound tRNA and G2252 in 23 S rRNA (12).

Here we present experiments using the 23 S rRNA-directed photoaffinity probe 811–803HHABA (Figure 1) to inves-

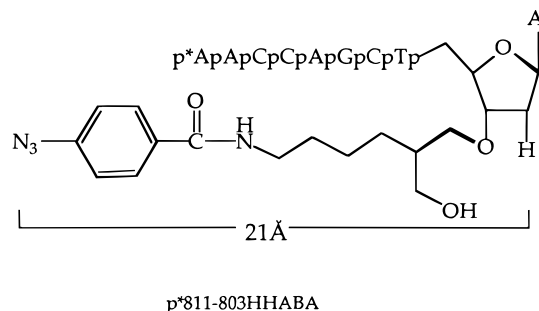


FIGURE 1: Photoaffinity probe 811–803HHABA. The distance between the photogenerated nitrene and the amine N of the nearest adenosine was determined to be 21 Å by molecular modeling with Quanta4.1 (Molecular Simulations, Inc.). The maximum distance between the nitrene and the 4-oxygen of U803 is 23 Å.

tigate the structural environment of ribosomal components within 23 Å of U803. As seen in Figure 1, the maximum distance between the nitrene generated upon photolysis of 811–803HHABA and the amine nitrogen of the 3'-terminal adenosine is 21 Å; the corresponding maximum distance between the nitrene and the 4-oxygen of U803 is 23 Å. Our results lead to the suggestion that nucleotides 803–811 are located between the back (solvent) side of the 50 S subunit and the peptidyl transferase center.

EXPERIMENTAL SECTION

Materials

Except as specified below, all materials were obtained as described (2–4).

Synthesis and Purification of Oligodeoxyribonucleotides. cDNA 811–803, having the sequence 5'-AACCAGCTA-3' and the corresponding mismatched oligonucleotide 5'-AAC-CTCCTA-3' (MM-cDNA 811–803; mismatches with the target sequence are in bold) were synthesized using phosphoramidite chemistry on a Milligen Biosearch Cyclone automated DNA synthesizer and deblocked according to the

[†] This work was supported by NIH Grant GM-53416, NSF Grant MCB-9118072, and an NSF predoctoral grant (RCD91-54685) to R.W.A.

* To whom inquiries should be addressed. Tel: 215 898 6330. FAX: 215 898 6330. E-mail: coopman@pobox.upenn.edu.

[‡] Present address: The Skaggs Institute for Chemical Biology, The Scripps Research Institute, 10550 N. Torrey Pines Rd., La Jolla, CA 92037.

¹ Abbreviations: p*811–803HHABA, N-[5-hydroxymethyl-6-(3'-pATCGACCAp*)]hexyl-p-azidobenzamide; HSAB, N-hydroxysuccinimidyl-4-azidobenzoate; PAGE, polyacrylamide gel electrophoresis; RP-HPLC, reverse-phase high-performance liquid chromatography; TP50, total protein from 50 S subunits; TND, 20 mM Tris-HCl (pH 7.6), 100 mM NaCl, 1 mM DTT; TBE, 90 mM Tris-borate, 2 mM EDTA.

manufacturer's protocol. 811–803HHABA, the photolabile 3'-O-(6-amino-2-hydroxymethyl)hexyl-*N*-*p*-azidobenzoate probe complementary to 23 S nucleotides 811–803, was synthesized as follows. 3'-Amino-modifier C7 CPG ((1-dimethoxytrityloxy-6-fluorenyl-methoxycarbonylamino-hexane-2-methyl-O-succinyl)-long chain alkylamino-CPG) was used to generate cDNA 811–803 derivatized at its 3'-end with a primary amine according to the protocol supplied by Glen Research (Sterling, VA). After deblocking and RP-HPLC purification, the 3'-amino derivatized cDNA 811–803 was reacted with HSAB to yield 811–803HHABA, using a procedure described earlier (3). The photolabile derivative was purified away from residual underivatized material by RP-HPLC on a C18 reverse-phase column using a linear 5–60% acetonitrile gradient in 0.1 M triethylamine-acetate (pH 7.6), and radiolabeled at the 5'-end with [γ - 32 P]-ATP using polynucleotide kinase (13) to produce p*811–803HHABA. cDNA 811–803 labeled at its 5'-end, p*811–803, was prepared similarly. Radiolabeled oligoDNA probes and primers were purified using Sep-pak (C-18) cartridges (13).

Methods

The following methods were carried out as described previously (2–5): Millipore filter binding assay of noncovalent probe/subunit complex formation, localization of photoincorporation sites within 23 S rRNA by RNase H, and reverse transcriptase analyses. Proteins were isolated from labeled 50 S subunits by acetic acid extraction and acetone precipitation in the usual fashion (14). Labeled proteins were identified by RP-HPLC (15), SDS–PAGE coupled with autoradiography (3–5), and, as needed, agarose antibody affinity chromatography (16).

Photoincorporation of p*811–803HHABA into 50 S Subunits. In a typical experiment, 150 pmol of 50 S subunits was incubated with 2–10 pmol of p*811–803HHABA in 75 μ L of TKM0.3 at 37 °C for 10 min and left on ice for 15 min. The MgCl₂ concentration was then increased to 10 mM, incubation was continued for an additional 2 h at 4 °C, and the sample was subjected to photolysis with 3000-Å lamps (Rayonet) for 4 min at 4 °C as described (3). Samples prepared for reverse transcriptase assays were photolyzed with nonradioactive 811–803HHABA at higher probe/subunit ratios (2:1 or 5:1).

RESULTS

Noncovalent Binding of cDNA p*811–803 to 50 S Subunits. Noncovalent binding of cDNA p*811–803 to 50 S subunits was determined using a Millipore filter binding assay (Figure 2). The results obtained are consistent with a minimal two-population binding model, in which one population of ribosomes binds the oligoDNA more tightly than does the other. Consideration of more complex models, in which the weaker binding population is composed of several subpopulations, is unwarranted by the data available. The minimal model may be described by eq 1. Here L is

$$\text{bound} = aR_tL[1/(K_{\text{app1}} + L) + \alpha/(K_{\text{app2}} + L)] \quad (1)$$

the concentration of unbound oligoDNA, a is the tighter-binding fraction of the total amount of 50 S subunits, R_t ,

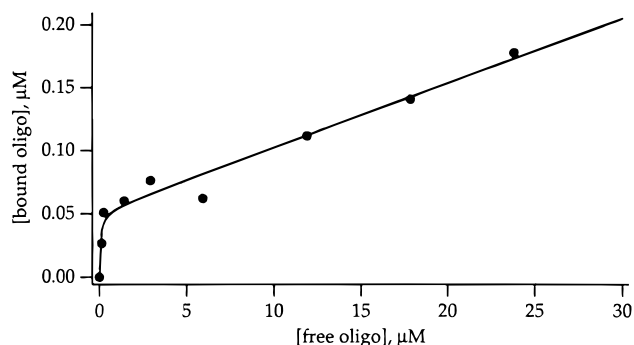


FIGURE 2: Millipore filter binding analysis of cDNA p*811–803 fit to a two-population model. 50 S subunits (15 pmol) were incubated with varying amounts of cDNA p*811–803 (400–500 cpm/pmol) and bound to Millipore filters. The amount of filter-bound oligonucleotide was determined by liquid scintillation counting of the dried filters. The total concentration of 50 S subunits in the binding mix was 0.6 μ M. The concentration of free oligo in the binding reaction was estimated from the difference of total (added) oligo concentration and bound oligo measured by counting the filters. Binding data were fit to eq 1, using the program IGOR (Wavemetrics, P. O. Box 2088, Lake Oswego, OR 97035).

and α is the weaker-binding fraction. The two populations bind oligoDNA with apparent dissociation constants K_{app1} and K_{app2} , respectively.

Fitting the binding data to this model yields the following parameter values used to generate the curve in Figure 2: K_{app1} , $0.07 \pm 0.06 \mu\text{M}$; a , 0.08 ± 0.01 ; and α/K_{app2} , $0.10 \pm 0.02 \mu\text{M}^{-1}$. Thus, 8% of the 50 S subunits bind cDNA 811–803 with high affinity.

RNase H cleavage of the complex between cDNA 811–803 and phenol/chloroform extracted 23 S rRNA produces a strong band at ~ 810 nt (Figure 3, lane 3), demonstrating that the probe binds to its target site. As expected, no 810-nt band results from RNase H cleavage of 23 S rRNA in the presence of MM-cDNA 811–803. Rather a 600-nt band is produced (lane 4), reflecting the partial complementarity of MM-cDNA 811–803 with nucleotides 615–621. The ~ 810 -nt band is formed upon incubation of RNase H with a mixture of 50 S subunits with either cDNA 811–803 or cDNA 811–803HHABA, but with much lower intensity than that seen in Figure 3 (data not shown), consistent with our finding that only a limited fraction of 50 S subunits binds tightly to cDNA 803–811.

Photoincorporation of p*811–803HHABA into 50 S Subunits. Photolysis experiments were typically conducted on solutions in which 50 S subunits were in stoichiometric excess over p*811–803HHABA (15–60-fold) in order to maximize incorporation from the high-affinity binding site (Figure 2). The percent of added probe photoincorporated into 23 S rRNA was estimated by liquid scintillation counting of the rRNA recovered from sucrose gradient centrifugation of labeled 50 S subunits. In a typical experiment, the percent of probe recovered with 23 S rRNA was as follows: without photolysis (background), 0.2%; with photolysis, 1.3%; with photolysis in the presence of cDNA 811–803, 0.4%; and with photolysis in the presence of MM-cDNA 811–803, 1.3%. The reduction in the presence of competing nonphotolabile cDNA 811–803 demonstrates the site specificity of the photoincorporation, while the lack of effect seen on addition of nonphotolabile MM-cDNA 811–803 is consistent with the site of labeling being the target site, rather than

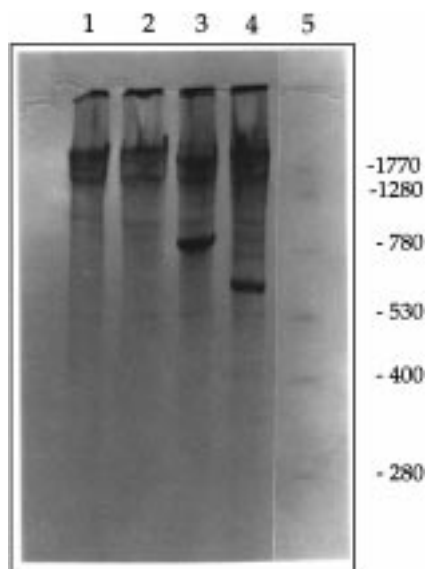


FIGURE 3: RNase H digestion of 23 S rRNA complexed with cDNA 811–803. Phenol/chloroform-extracted and ethanol-precipitated 23 S rRNA (25 pmol) was cleaved with RNase H (2 units) in the presence of either cDNA 811–803 or MM-cDNA 811–803 (50 pmol) in 10 μ L of TND buffer with 10 mM $MgCl_2$ for 30 min at 32 $^{\circ}C$. The cleavage products were electrophoresed on a 3.5% acrylamide/0.18% bis(acrylamide)/7 M urea gel made up in TBE buffer and visualized with methylene blue. Lane 1: no RNase H, no added cDNA. Lane 2: RNase H, no added cDNA. Lane 3, with cDNA 811–803. Lane 4, with MM-cDNA 811–803. Lane 5, RNA size markers, with sizes (in nt) indicated to the right of the gel.

some other site on the 50 S subunit that binds p*811–803HHABA with high affinity. The corresponding photoincorporation numbers for TP50, as estimated from radioactivity coeluting with 50 S protein on RP-HPLC analysis: with photolysis, 2.0%; with photolysis in the presence of cDNA 811–803, 1.1%; and with photolysis in the presence of MM-cDNA 811–803, 1.9%. No direct estimate was made in the absence of photolysis, but from SDS–PAGE analysis this value was negligible.

Localization of p*811–803HHABA Photoincorporation Sites in 23 S rRNA. All photoincorporation of p*811–803HHABA into 50 S RNA took place solely into 23 S rRNA; no incorporation into 5 S rRNA was observed, as shown by the absence of radioactivity in the region of 120–130 nts on urea–PAGE analysis (Figure 4, lanes 1 and 3). RNase H cleavage of labeled 23 S rRNA produces a ^{32}P -labeled fragment at approximately 820 nt (Figure 4, lanes 4 and 6), indicating that, under the conditions of the assay, the hybrid between p*811–803HHABA and 23 S rRNA is re-formed as a substrate for RNase H, and that 23 S rRNA labeling is limited to nucleotides 5' to the 811–803 cleavage site.

To further localize incorporation sites, 23 S rRNA extracted from labeled 50 S subunits was subjected to RNase H cleavage in the presence of several cDNAs, and the resulting fragments were also analyzed by urea–PAGE and autoradiography. The apparent sizes of labeled fragments, as determined by comparison with RNA size markers, are typically 10–20 nts larger than would be expected for calculated unlabeled fragments, due to both the size of the photoincorporated probe itself (9 nts) and the “frayed” ends that sometimes result from incomplete RNase H digestion.

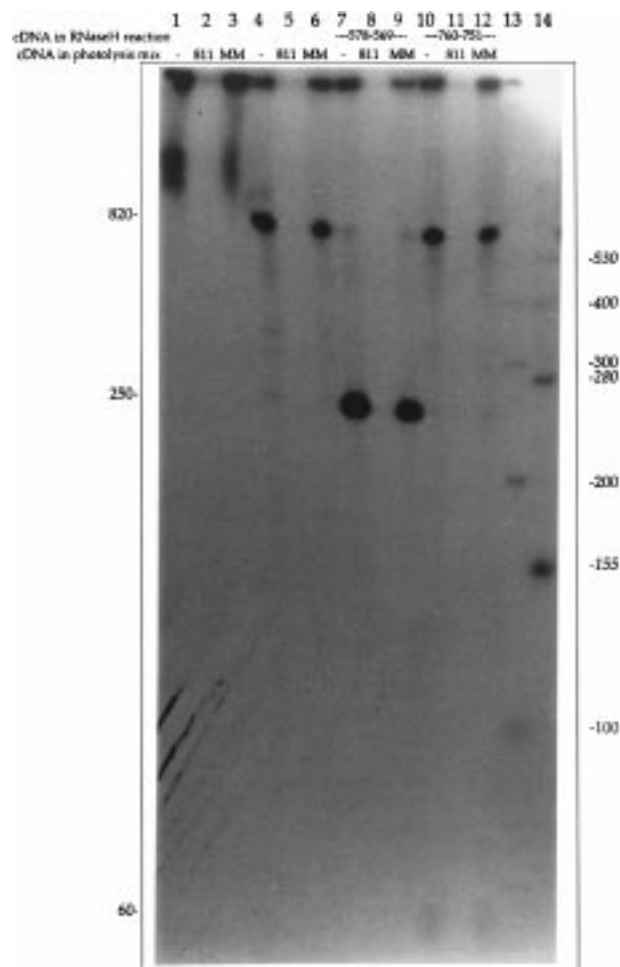


FIGURE 4: RNase H digestion of p*811–803HHABA-labeled 23 S rRNA. Labeled 23 S rRNA (8 pmol) prepared from 50 S subunits photolyzed in the presence of p*811–803HHABA and separated from non-incorporated material by sucrose gradient centrifugation was incubated with 16 pmol of the indicated cDNA probe in 10 μ L of TND buffer with 10 mM $MgCl_2$ and digested with 2 units of RNase H. The cleavage products were electrophoresed on a 5% polyacrylamide/0.25% bis(acrylamide)/7 M urea gel made up in TBE buffer. Radioactive fragments were visualized by autoradiography. Photolabeling experiments were carried out in the absence of added cDNA (lanes 1, 4, 7, and 10) or in the presence of a 10-fold (over ribosomes) excess of cDNA 811–803 (lanes 2, 5, 8, and 11) or MM-cDNA 811–803 (lanes 3, 6, 9, and 12). Lanes 1–3: labeled 23 S rRNA in the absence of RNase H. Samples for lanes 4–12 were digested with RNase H. Lanes 4–6: no added cDNA. Lanes 7–9: with cDNA 578–569. Lanes 10–12: with cDNA 760–751. Lane 13: DNA size markers. Lane 14: RNA size markers, with sizes (in nt) indicated to the right of the gel. RNA sizes are italicized. Sizes to the left of the gel correspond to approximate sizes of labeled fragments produced by RNase H cleavage.

The addition of cDNA 578–569 produces an intense band at 250 nt, with virtually complete disappearance of the 820-nt band and no appearance of a new band at approximately 590 nt (Figure 4, lanes 7–9). Addition of cDNA 760–751 yields only a weak band at 60 nt, leaving most of the 820-nt band intact (Figure 4, lanes 10–12), indicating that the hybrid formed between nucleotides 751–760 and the corresponding cDNA is not a good substrate for RNase H cleavage. These results demonstrate that there is a site or sites of labeling between nucleotides 569/578 and 803/811, that is likely further restricted to between 751/760 and 803/811. As expected from the absence in lanes 4–6 of any bands larger

that 820 nt, cDNAs complementary to nucleotides 1051–1060, 1391–1400, 1741–1750, 2100–2116, 2368–2377, 2497–2505, and 2655–2662, incubated individually and in pairs with labeled 23 S rRNA, did not produce labeled fragments on digestion with RNase H other than those ascribable to labeling at or near nts 803/811 (data not shown).

To identify labeled nucleotides in the region 751/760 to 803/811, labeled 23 S rRNA purified by SDS–sucrose gradient centrifugation was used as a substrate for AMV–reverse transcriptase in the presence of primer cDNA 875–856. In this experiment, much higher ratios of photoaffinity probe 811–803HHABA:50 S (2:1 and 5:1) were used than in the RNase H experiments, in which the corresponding ratio was $\leq 0.07:1$. This was done in order to maximize probe incorporation and increase the visibility of autoradiographic bands due to primer extension stops or pauses. PAGE and autoradiographic analysis of the extension products (Figure 5) showed U803 to be the major photoincorporation-dependent stop in the region 747–836, thus identifying A802 as the major site of photoincorporation into 23 S rRNA. The minor stops at G801, A802, G805, and C806 might indicate photoincorporation into some neighboring sites as well, or may be stuttering artifacts (17).

50 S Proteins Site-Specifically Labeled by p*811–803HHABA. Labeled proteins were for the most part identified by combining RP–HPLC and SDS–PAGE analyses. When this combination proved insufficient, agarose antibody affinity chromatography was used additionally.

RP–HPLC analysis of TP50 extracted from labeled 50 S subunits produced a total of seven labeled peaks, A–G (Figure 6), of which D is clearly the largest. Added cDNA 811–803 decreased labeling of peaks E–G more than addition of MM–cDNA 811–803 (Table 1), making it clear that one or more proteins in each of these peaks are labeled site-specifically. In contrast, such differential labeling is less obvious for peaks A–D. Furthermore, peak A was observed even in samples which had not been photolyzed. Accordingly, peak A was not further analyzed.

We previously have shown that ribosomal proteins covalently labeled with oligoDNAs elute on RP–HPLC with or close to unmodified protein, and migrate in SDS–PAGE with apparent masses approximately equal to the sum of the masses of the labeled protein and the attached oligoDNA (2–5), which in this case is 3.2 kDa. SDS–PAGE and autoradiographic analysis was performed on labeled TP50, revealing the presence of eight labeled bands denoted i–viii (Figure 7). Consistent with RP–HPLC analysis, the intensity of some bands (e.g., ii, iii) is decreased much more in the presence of added cDNA 811–803 than of added MM–cDNA 811–803, while such differences are less marked for others (e.g., bands i and viii). We return to this point below.

SDS–PAGE analysis was performed on RP–HPLC fractions corresponding to peaks B–G (Figure 8). By considering the apparent molecular weights of labeled and unlabeled proteins on the SDS–PAGE gel and the well-established elution order of unlabeled proteins on the RP–HPLC gradient employed, we were able to identify L27, L2, L13, L21, and L20 as labeled proteins (Table 2). Confirmation that bands vi, iv, and iii correspond to labeled proteins L28, L17, and L15, respectively, was provided by agarose antibody affinity chromatography analysis of peaks C, E, and F (Figure 9). The most difficult identification concerned band iii from peak

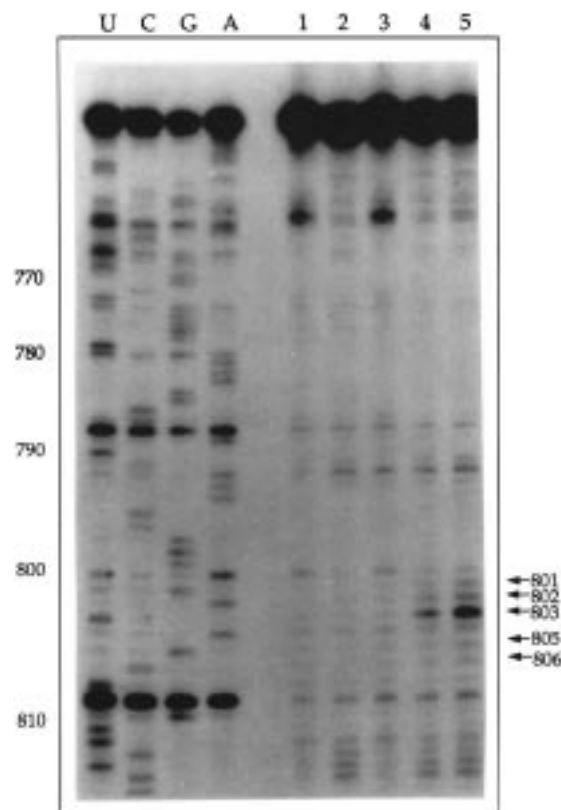


FIGURE 5: Reverse transcriptase analysis of p*811–803HHABA-labeled 23 S rRNA. Photoincorporation was performed using 75 pmol of 50 S subunits in a reaction volume of 75 μ L; the primer used was cDNA 875–856. Lane 1: no photolysis, no 811–803HHABA probe. Lane 2: photolyzed 50 S subunits, no probe. Lane 3: no photolysis, with 750 pmol of probe. Lane 4: photolyzed with 150 pmol of probe. Lane 5: photolyzed with 375 pmol of probe. Lanes U, C, G, and A are sequencing products generated from control (nonphotolyzed) 23 S rRNA in the presence of ddATP, ddGTP, ddCTP, and ddTTP, respectively. Nucleotides at which pauses or stops induced by photoincorporation of 811–803HHABA are observed are indicated.

F, since L15 and L16 are not well-resolved by either RP–HPLC or SDS–PAGE and have similar molecular masses (15.0 and 15.3 kDa, respectively). In fact, while the data in Figure 9 do show L15 to be the highest labeled protein in peak F, some labeling of L16 is not excluded. Last, we were unable to identify minor band vii; possible candidates include L29, L30, L32, and L33.

On the basis of both the extent of labeling and the decrease in such labeling in the presence of added cDNA 811–803, the major site-specifically labeled proteins by p*811–803HHABA are L15, L17, and L20. L13 and L21 are also labeled site-specifically, but to lesser extents. L2, L27, and L28 are major labeled proteins, but because added cDNA 811–803 only partially decreases incorporation into these proteins, we do not consider them to be clearly labeled from the target site. Also not considered as being labeled from the target site is L31, as the corresponding minor labeled band (band viii from peak B) shows no apparent reduction in intensity in the presence of added cDNA 811–803 (Figure 8).

DISCUSSION

The results presented here demonstrate that proteins L13, L15, L17, L20 and L21 are all within 23 Å of nucleotide U803. Confidence that photolabeling of these proteins arises

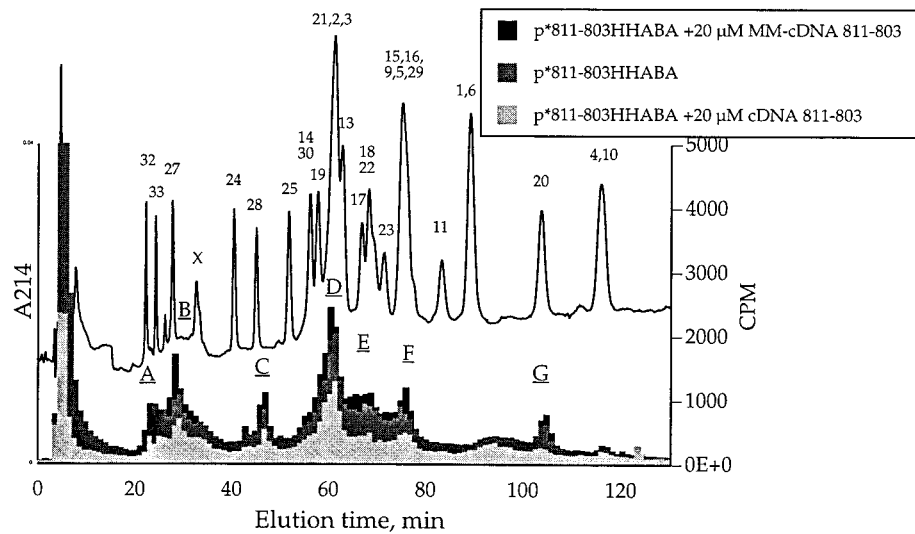


FIGURE 6: RP-HPLC of p*811–803HHABA-labeled TP50. The photolysis reaction mixture (total volume, 75 μ L) contained 50 S subunits (150 pmol) and p*811–803 HHABA (10 pmol) in the absence or presence (1500 pmol) of added cDNA 811–803 or MM-cDNA 811–803. For each analysis, proteins were extracted from photolyzed subunits with 67% acetic acid, precipitated with 5 volumes of acetone, redissolved in 200 μ L of 0.1% TFA, applied to a SynChropak RP-P reverse-phase C18 column, and eluted at a flow rate of 0.7 mL/min with a 120-min 15–45% convex acetonitrile gradient containing 0.1% TFA.

Table 1: Photoincorporation of p*811–803HHABA into 50 S Proteins^a

RP-HPLC peak ^b	% of probe incorporated	rel incorporation ^c	
		on addn of cDNA 811–803 ^c	on addn of MM-cDNA 811–803 ^c
A	0.23 \pm 0.07	0.6 \pm 0.2	0.9 \pm 0.3
B	0.33 \pm 0.04	0.7 \pm 0.2	0.9 \pm 0.2
C	0.12 \pm 0.01	0.7 \pm 0.2	1.1 \pm 0.3
D	0.70 \pm 0.13	0.61 \pm 0.07	0.9 \pm 0.1
E	0.27 \pm 0.03	0.40 \pm 0.06	0.9 \pm 0.1
F	0.23 \pm 0.04	0.34 \pm 0.08	0.95 \pm 0.05
G	0.13 \pm 0.04	0.19 \pm 0.05	1.1 \pm 0.1
no. of determinations	5	4	4

^a Probe:50 S subunit ratio was 2–2.5 pmol of probe:150 pmol of subunits in 75 μ L of reaction mixture. ^b See Figure 6. ^c Incorporation in the absence of added cDNA (1500 pmol) is 1.00.

from the oligoDNA probe bound to the target site comes from three principal lines of evidence. First, cDNA 811–803 binds to its target site in 23 S rRNA, as shown by the release of an 820-nt fragment on digestion of the cDNA 811–803:23 S rRNA complex. Second, labeling of 23 S rRNA on photolysis of 50 S subunits in the presence of p*811–803HHABA occurs site-specifically between nucleotides 751/760 and 803/811 as demonstrated by RNase H assay using RNA labeled at a low probe:subunit ratio; within this region, nucleotide A802, immediately adjacent to the target site, is the major site of incorporation, as identified by the reverse transcriptase assay on RNA samples labeled at much higher probe:subunit ratios. Third, labeling of each of the proteins L13, L15, L17, L20, and L21 was much decreased when photolysis was carried out in the presence of the competing cDNA 811–803, but was not affected in the presence of MM-cDNA 811–803, which mimics the cDNA except for two mismatched bases designed to prevent binding to the target site. The latter is in contrast to the only modest reduction in the labeling of proteins L2, L27, and L28 on addition of cDNA 811–803, and the lack of reduction of L31 labeling. These differing results demon-

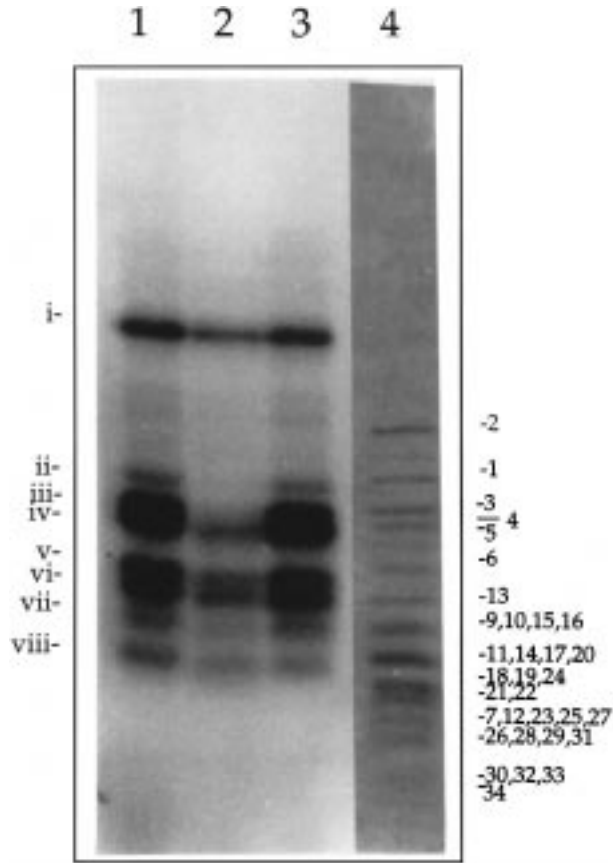


FIGURE 7: SDS-PAGE of p*811–803HHABA-labeled TP50. TP50 from 50 S subunits (150 pmol) photolabeled with p*811–803HHABA in the absence or presence (1500 pmol) of cDNA 811–803 or MM-cDNA 811–803 was extracted with 67% acetic acid, precipitated with 5 volumes of acetone, and analyzed on an 18% acrylamide/0.10% bis(acrylamide) gel made up in 0.75 M Tris-HCl (pH 8.8)/0.1% SDS. Lane 1: subunits photolyzed with no added cDNA. Lane 2: with cDNA 811–803. Lane 3, with MM-cDNA 811–803. Lane 4: TP50 stained with Coomassie Blue.

strate that specific site labeling can be distinguished from nonspecific labeling by its sensitivity to added cDNA complementary to the target site.

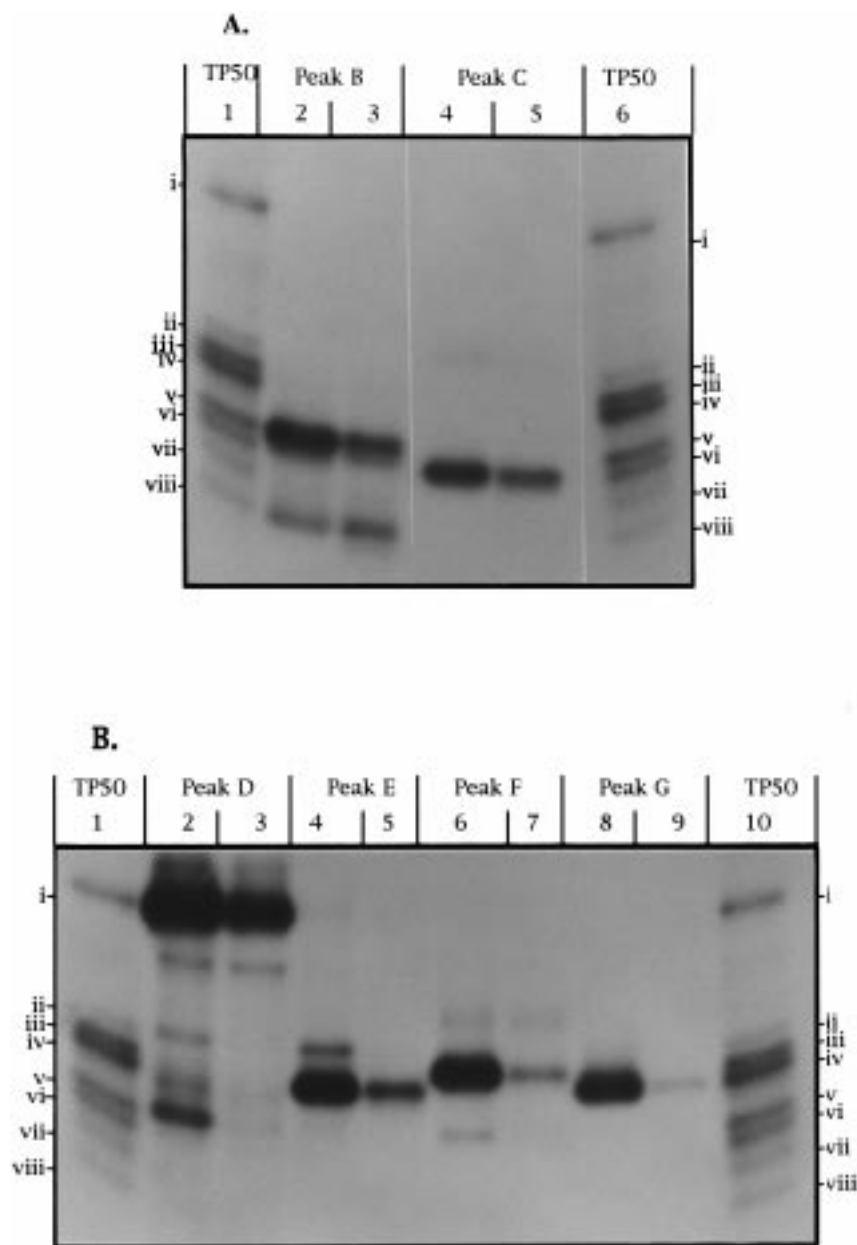


FIGURE 8: SDS-PAGE analysis of RP-HPLC peaks containing p*811–803HHABA-labeled 50 S proteins. Labeled 50 S proteins were separated by RP-HPLC as in Figure 6 and electrophoresed on an 18% acrylamide/0.10% bis(acrylamide) gel made up in 0.75 M Tris-HCl (pH 8.8)/0.1% SDS. (A) Lanes 1 and 6: p*811–803-labeled TP50. Lanes 2 and 4: peaks B and C, respectively, for the sample labeled in the absence of added cDNA 811–803. Lanes 3 and 5: peaks B and C, respectively, for the sample labeled in the presence of added cDNA 811–803. (B) Lanes 1 and 10: p*811–803-labeled TP50. Lanes 2, 4, 6, and 8: peaks D, E, F, and G, respectively, for the sample labeled in the absence of added cDNA 811–803. Lanes 3, 5, 7, and 9: peaks D, E, F, and G, respectively, for the sample labeled in the presence of added cDNA 811–803.

It is of interest to compare our results to other studies of internal 50 S structure. The best current model for the spatial arrangement of proteins in the 50 S particle remains that of Wallacek et al. (19), which is based on a combination of immunoelectron microscopy and cross-linking results. Four of the specifically labeled proteins in this work, L13, L17, L20, and L21, form a tight cluster in the Wallacek et al. model (Table 3), on the “back” side of the 50 S subunit, facing away from the 30 S subunit. Protein L15, which has been implicated as being at or near the peptidyl transferase center (20), though not a part of this cluster, is not unreasonably far from L21 (centers of mass separated by 66 Å, Table 3) to be labeled by 811–803HHABA from a common site.

The mutual proximity of proteins L13, L15, L17, and L21 is also suggested by their each having been photo-cross-linked to tRNAs derivatized with aryl azides. L15 was labeled by a P-site bound tRNA in which the 3′-terminal adenosine is replaced by 2-azidoadenosine (21). In experiments employing tRNAs in which aryl azide groups are attached to guanosines widely distributed over the whole molecule, proteins L13 and L17 are labeled by tRNAs bound to the A-site, and proteins L15 and L21 are labeled by tRNAs bound to the P-site (22, 23). Our results thus complete a logical triangle, directly linking two proteins (L15 and L21) and a region of 23 S rRNA (803–811) that have each been separately implicated in the binding of the tRNA to the P-site (9). Together with the Wallacek et al. model and the results

Table 2: SDS-PAGE Analysis of RP-HPLC Peaks

RP-HPLC peak ^a	bands ^b	apparent mass of band (kDa) ^c	labeled protein identified ^d	effect of added cDNA 811–803 ^e	mass of unlabeled protein (kDa)	
					apparent ^c	calcd ^f
B	v	13.9	L27	↓	11.0	9.0
C	vi	12.5	L28	↓	10.1	8.9
D	i	33.9	L2	↓	29.7	29.8
	ii	19.7	L13	↓↓	16.0	16.0
	iv	16.3	L17	↓↓	12.9	14.4
	v	14.5	L21	↓↓	11.0	11.6
E	ii	19.7	L13	↓↓	16.0	16.0
	iv	16.3	L17	↓↓	12.9	14.4
F	iii	17.9	L15	↓↓	14.3	15.0
G	iv	17.1	L20	↓↓	13.5	13.4

^a See Figure 6. ^b In the case of multiple bands, bolded one(s) is (are) most intense. ^c Calculated from migration on SDS-PAGE analysis, using a standard curve of electrophoretic migration distance vs log of molecular mass. ^d See Results and Figure 9. ^e ↓, small decrease in labeling; ↓↓, large decrease in labeling. ^f Reference 18.

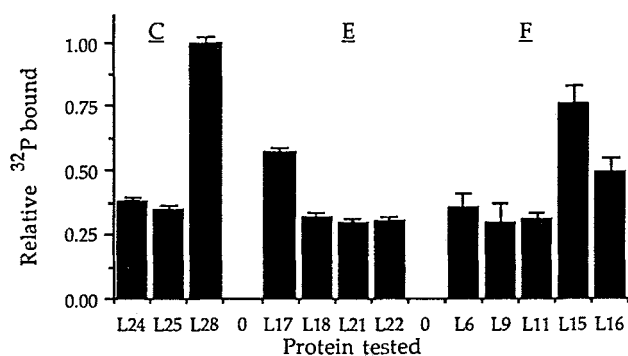


FIGURE 9: Antibody identification of HPLC-purified labeled proteins. Agarose antibody affinity chromatography analysis of RP-HPLC peaks C, E, and F, as indicated.

Table 3: Selected Protein-Protein Distances (Å) in the Model of Walliczek et al. (19)

	L13	L15	L17	L20
L15	85			
L17	35	118		
L20	39	95	52	
L21	29	66	59	31

of Hill et al. (9) suggesting a specific interaction between nucleotides 803–811 and the 3'-end of P-site bound tRNA, they point to a location for nucleotides 803–811 between proteins L21 and L15, on the side of the L13-L17-L20-L21 cluster that points from the back of the 50 S particle toward the peptidyl transferase center, as depicted in Figure 10.

Such a placement is consistent with the results of earlier studies by us and others. Protein L13 is also labeled by a photolabile cDNA probe targeted to the 2475 loop in domain V (5), which is connected by a stem to the domain V central loop at the peptidyl transferase center (20). In addition, nucleotides in domain II on either side of 803–811, namely, 739–748 and 979–981/983–984, have been found to cross-link to sites at or near the domain V central loop [to 2609–2618 (24) and to G2029 (25), respectively], and nucleotide A750 is cross-linked to a growing peptide chain, 6–14 amino acids long, bound through tRNA to the ribosome (26).

Finally, proteins L15 and L17 are also labeled by a photolabile cDNA probe targeted to the α -sarcin region in domain VI (6), suggesting a proximity between nucleotides

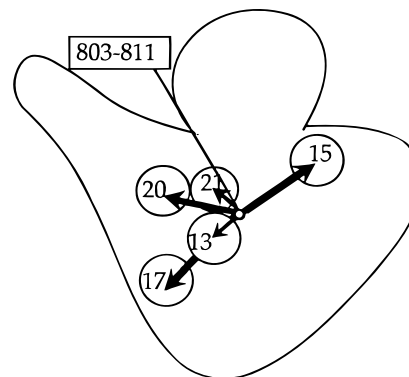


FIGURE 10: Proposed location of 23 S rRNA nucleotides 803–811. Major specifically labeled proteins L15, L17, and L20 and minor specifically labeled proteins L13 and L21 as localized on the 50 S subunit interface surface according to Walliczek et al. (19).

803–811 and this region. While this suggestion is novel, it is hardly surprising, given the strong evidence for the proximity to the domain V central loop of both nucleotides 803–811 and the α -sarcin region (3, 6, 27).

ACKNOWLEDGMENT

We acknowledge with thanks Ms. Nora Zuño for excellent technical assistance in several aspects of this work, Dr. Parimi Muralikrishna for helpful suggestions, and Dr. Richard Brimacombe for carrying out the agarose antibody affinity chromatography analyses.

REFERENCES

- Cooperman, B. S., Muralikrishna, P., and Alexander, R. W. (1993) in *The Translational Apparatus* (Nierhaus, K. H., Subramanian, A. R., Erdmann, V. A., Franceschi, F., and Wittman-Liebold, B., Eds.) pp 465–476, Plenum Press, New York.
- Alexander, R. W., Muralikrishna, P., and Cooperman, B. S. (1994) *Biochemistry* 33, 12109–12118.
- Muralikrishna, P., and Cooperman, B. S. (1991) *Biochemistry* 30, 5421–5428.
- Muralikrishna, P., and Cooperman, B. S. (1994) *Biochemistry* 33, 1392–1398.
- Muralikrishna, P., and Cooperman, B. S. (1995) *Biochemistry* 34, 115–121.
- Muralikrishna, P., Alexander, R. W., and Cooperman, B. S. (1997) *Nucleic Acids Res.* 25, 4562–4569.
- Brimacombe, R. (1995) *Eur. J. Biochem.* 230, 365–383.
- Green R., and Noller, H. F. (1997) *Annu. Rev. Biochem.* 66, 679–716.
- Hill, W. E., Tassanakajohn, A., and Tappich, W. E. (1990) *Biochim. Biophys. Acta* 1050, 45–50.
- Barta, A., Steiner, G., Brosius, J., Noller, H. F., and Kuechler, E. (1984) *Proc. Natl. Acad. Sci. U.S.A.* 81, 3607–3611.
- Gutell, R., and Fox, G. (1988) *Nucleic Acids Res.* 16, r175–r269.
- Samaha, R. R., Green, R., and Noller, H. F. (1995) *Nature* 377, 309–314.
- Sambrook, J., Maniatis, T., and Fritsch, E. F. (1989) *Molecular Cloning: A Laboratory Manual* 2nd ed., pp 11–39, Cold Spring Harbor Laboratory, Cold Spring Harbor, NY.
- Kerlavage, A. R., and Cooperman, B. S. (1986) *Biochemistry* 25, 8002–8010.
- Kerlavage, A. R., Weitzmann, C. J., and Cooperman, B. S. (1984) *J. Chromatogr.* 317, 201–212.
- Gulle, H., Hoppe, E., Osswald, M., Greuer, B., Brimacombe, R., and Stoffler, G. (1988) *Nucleic Acids Res.* 16, 815–832.
- Denman, R., Colgan, J., Nurse, K., and Ofengand, J. (1988) *Nucleic Acids Res.* 16, 165–178.
- Giri, L., Hill, W. E., Wittmann, H. G., and Wittmann-Liebold, B. (1984) *Adv. Protein Chem.* 36, 1–78.

19. Walieczech, J., Schüler, D., Stöffler-Meilicke, M., Brimacombe, R., and Stöffler G. (1988) *EMBO J.* 7, 3571–3576.
20. Cooperman, B. S., Weitzmann, C. J., and Fernández, C. L. (1990) in *The Ribosome: Structure, Function, and Evolution* (Hill, W. E., Dahlberg, A., Garrett, R. A., Moore, P. B., Schlessinger, D., and Warner, J. R., Eds.) pp 491–501, American Society for Microbiology, Washington, DC.
21. Wower, J., Hixson, S. S., and Zimmermann, R. A. (1989) *Proc. Natl. Acad. Sci. U.S.A.* 86, 5232–5236.
22. Vladimirov, S. N., Graifer, D. M., Karpova, G. G., Semenov, Y. P., Makhno, V. I., and Kirillov, S. V. (1985) *FEBS Lett.* 181, 367–372.
23. Graifer, D. M., Babkina, G. T., Matasova, N. B., Vladimirov, S. N., Karpova, G. G., and Vlassov, V. V. (1989) *Biochim. Biophys. Acta* 1008, 146–156.
24. Stiege, W., Glotz, C., and Brimacombe, R. (1983) *Nucleic Acids Res.* 11, 1687–1706.
25. Döring, T., Greuer, B., and Brimacombe, R. (1991) *Nucleic Acids Res.* 19, 2517–3524.
26. Stade, K., Jünke, N., and Brimacombe, R. (1995) *Nucleic Acids Res.* 23, 2371–2380.
27. Joseph, S., and Noller, H. F. (1996) *EMBO J.* 15, 910–916.

BI972280+